Article
Vol. 24, No. 2, p. 177–193, April 2020
https://doi.org/10.1007/s12303-019-0018-7
pISSN 1226-4806 eISSN 1598-7477
Geosciences Journal GJ

Depositional environments of redox-sensitive trace elements in the metalliferous black slates of the Okcheon Metamorphic Belt, South Korea

Juyoung Jeon, Dongbok Shin*, and Heonkyung Im

Department of Geoenvironmental Sciences, Kongju National University, Gongju, Chugnam 32588, Republic of Korea

ABSTRACT: Metalliferous black slates consisting of black slates and interbedded coaly slates in the Okcheon Metamorphic Belt of South Korea were analyzed for redox-sensitive trace elements and rare earth elements (REEs) to examine their depositional conditions. Our data show that the coaly slates have elevated concentrations of redox-sensitive trace metals (U, V, Mo, and Cr), low Mn contents, high V/(V + Ni), V/Cr, and U/Th ratios, and high total organic carbon (TOC) contents. A general tendency of positive correlation between TOC and trace metals was established. The results suggest that the coaly slates were developed under a strongly reducing environment, while the black slates were deposited under a suboxic-oxic condition. The REE patterns of the coaly slates typically show positive Eu and negative Ce anomalies compared to the North American Shale Composite reference and they are essentially inherited from submarine hydrothermal fluids under high temperature reducing condition. The enrichment of the redox-sensitive elements including V (up to 3,564 ppm) and Mo (up to 358 ppm) may have been controlled by direct hydrothermal input of metals into the rift basin from hydrothermal vents, proximal from the vent sites, as supported by textural evidences, and the metals could have been fixed from seawater by means of scavenging process via exhalative oxide particles in a hydrothermal plume. The sorption of metals from seawater under anoxic conditions into organic-rich sediments occurred as well. The metal enrichments in the black slates seem to have been achieved in somewhat similar way to black shales in South China.

Key words: redox-sensitive elements, metalliferous black slates, hydrothermal fluids, Okcheon Metamorphic Belt

Manuscript received April 14, 2019; Manuscript accepted July 9, 2019

1. INTRODUCTION

Metalliferous black shales that include Mo, Ni, As, Zn, Cu, and U have been reported from various parts of the world and they show distinct geochemical signatures reflecting their depositional environments. Metalliferous black slates in the Okcheon Metamorphic Belt (OMB) of South Korea have drawn attention for their potential mineralization of U as well as other metallic elements. Many studies have focused on the tectonics, stratigraphy, mineralogy and geochemistry related to uranium mineralization in the OMB (e.g., Lee et al., 1986; Kim, 1989; Lee and Lee, 1997; Jeong and Lee, 2001; Jeong, 2006). It has been shown that the metalliferous black slates are characterized by a high content of trace elements such as Ba, V, Mo, and U (Kim, 1989; Kim et al., 2015), and based on mineralogy and geochemistry, Jeong (2006) also interpreted that the metalliferous black slates of the OMB are comparable to the metalliferous black shales in the South China block.

Recently, it has been recognized that the metalliferous black slates in the OMB are interbedded with coaly slates, which are more enriched with U and other metallic elements than the surrounding black slates (Shin and Kim, 2011; Jo et al., 2013). However, previous studies have not divided the two rock types based on their petrography and geochemistry in their genetic consideration. Shin et al. (2016) attempted to clarify the differences in U minerals and S isotope compositions of the two rock types and discussed their genetic environments. However, so far, redox-sensitive elements contained in the metalliferous black slates have not been discussed in detail to examine their depositional conditions. The concentrations and distributions of redox-sensitive elements have been widely used to constrain the depositional condition of black shales (e.g., Shields and Stille, 2001; Pasava et al., 2008; Kunzmann et al., 2015). Thus, this study focuses on the

*Corresponding author:
Dongbok Shin
Department of Geoenvironmental Sciences, Kongju National University, Gongju, Chugnam 32588, Republic of Korea
Tel: +82-41-850-8509, Fax: +82-41-850-8953, E-mail: shin@kongju.ac.kr

geochemistry of redox-sensitive trace elements, total organic carbon (TOC), and rare earth elements (REEs) in an attempt to constrain the depositional conditions of the metalliferous black slates in the OMB by comparing the two constituent rock types, black slates and coaly slates. The results are also compared with those of the Early Cambrian polymetallic black shales in South China Block, which has been tectonically correlated with the OMB.

2. GEOLOGIC SETTING AND PETROGRAPHY

The OMB is a NE-trending belt that forms the boundary

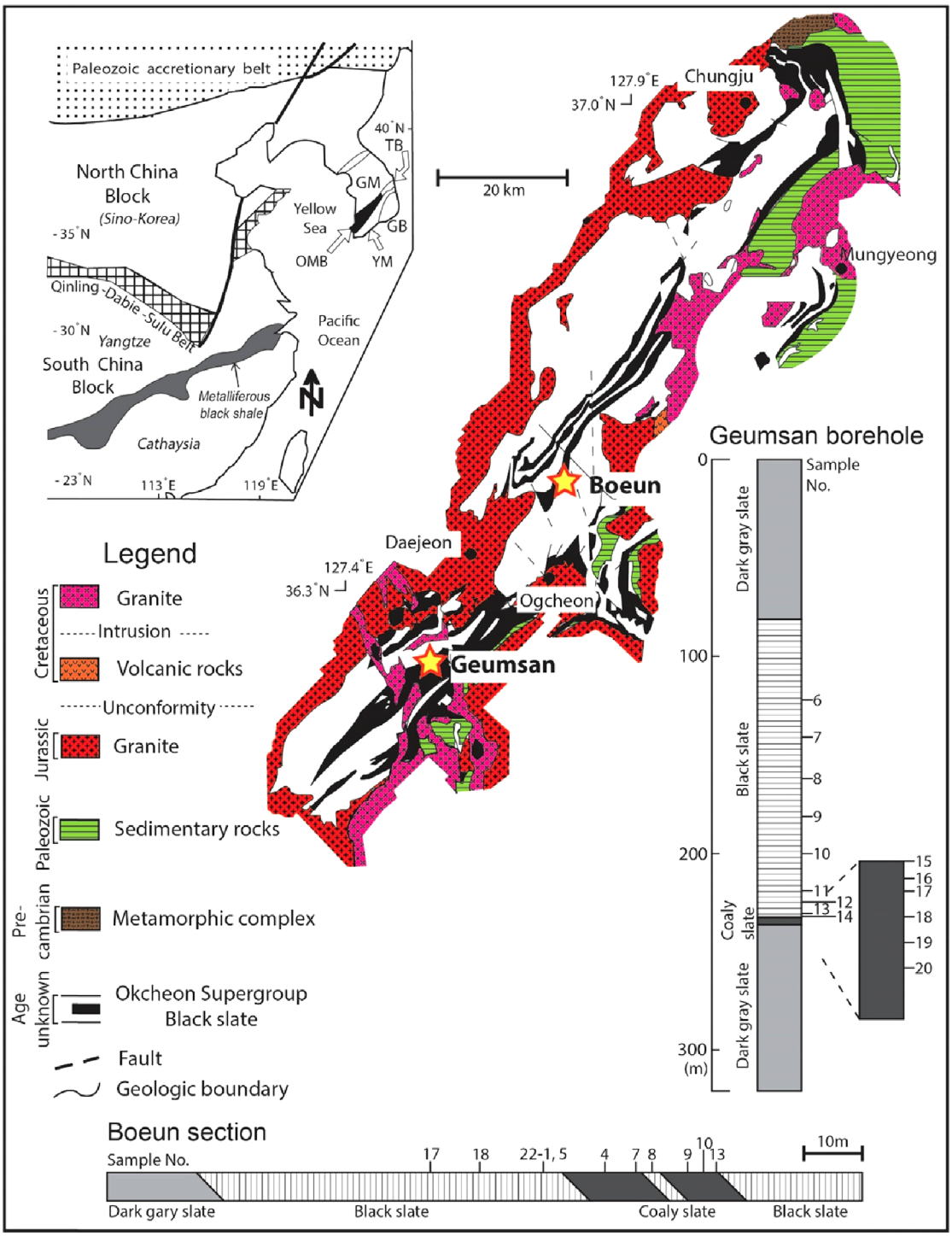

Fig. 1. Distribution of the black slates in the OMB and two locations (Boeun, Geumsan) of outcrops investigated in this study with tectonic map of northeast Asia (modified from Cheong et al., 2003). GM: Gyeonggi Massif, TB: Taebaegsan Basin, YM: Yeongnam Massif, GB: Gyeongsang Basin.

between two Archean to early Proterozoic basements, the Gyeonggi massif to the northwest and the Yeongnam massif to the southeast, on the Korean Peninsula (Cluzel et al., 1990) (Fig. 1). The belt has been suggested to be an extension of the Huanan aulacogen within the South China Craton (Chang, 1996; Ree et al., 2001; Chough, 2013) or an extension of the Hida Belt in Japan (Hiroi, 1983; Suzuki and Adachi, 1994). Bimodal distribution of metavolcanics has been suggestive of a rift basin origin (Cluzel et al., 1990; Kwon and Lan, 1991; Kang et al., 2012).

The OMB is dominantly composed of pelitic and psammitic rocks with local occurrences of metavolcanic rocks, quartzite, conglomerate, and calc-silicate and carbonate rocks (Chough, 2013). These rocks have undergone polyphase deformation during low- to medium-grade tectonometamophic episodes, which have contributed to the formation of a fold-thrust zone, defined by SE-verging, ductile, and stacking nappes (Cluzel et al., 1990). Intrusion of Mesozoic granitoids is prevalent throughout the OMB, resulting in low-grade thermal metamorphism in the region (Min and Cho, 1998). Isotopic ages have constrained the depositional and metamorphic ages of the metasedimentary rocks of the OMB. A U-Pb zircon age of 756 Ma obtained from metarhyolite was interpreted to represent Neoproterozoic rift-related volcanism in the OMB (Lee et al., 1998). Pb-Pb whole rock analyses for the metalliferous black slates yielded ages of 283–291 Ma, indicating that the peak metamorphism occurred during the early Permian (Cheong et al., 2003).

The metalliferous black slates are relatively well developed and extend for over 100 km in a NE-direction (Fig. 1). They commonly include coaly slates, which are more carbonaceous and metalliferous than the surrounding rocks and form a layer approximately 10–40 m thick. The black slates, as a constituent part, generally exhibit a platy and schistose texture (Fig. 2a), but are locally massive. Quartz and calcite veinlets about 1 mm wide and disseminated or veinlet sulfide minerals are also common (Fig. 2d). Major constituent minerals are quartz, muscovite, pyrite, and coaly materials. Tremolite, chlorite, biotite, epidote, calcite, and orthoclase are also present as minor phases (Figs. 3a–d). Pyrite commonly shows subhedral or anhedral form and occurs as a disseminated mineral or as veinlets parallel to the schistosity of the black slates (Figs. 3a and c). Randomly-oriented quartz veinlets, which cut the schistosity of the black slates, are also developed near the contact with the coaly slates.

The coaly slates with abundant carbonaceous materials are conspicuously darker than the surrounding black slates (Fig. 2). They commonly form a sharp contact with the black slates, but show gradual variations locally. Brecciated and flow textures with subparallel-oriented minerals including quartz and carbonaceous materials are also developed (Fig. 2e). In addition, unlike the black slates, nodular quartz veins accompanying massive sulfide minerals occur intermittently (Figs. 2b and c). In the coaly slates, coal materials, quartz, and pyrite are more abundant than in the black slates, and muscovite, phlogopite, apatite, chlorite, calcite, pyrrhotite and sphalerite are present as minor phases (Figs. 3e–i).

U mineralization is characterized by the occurrence of uraninite,

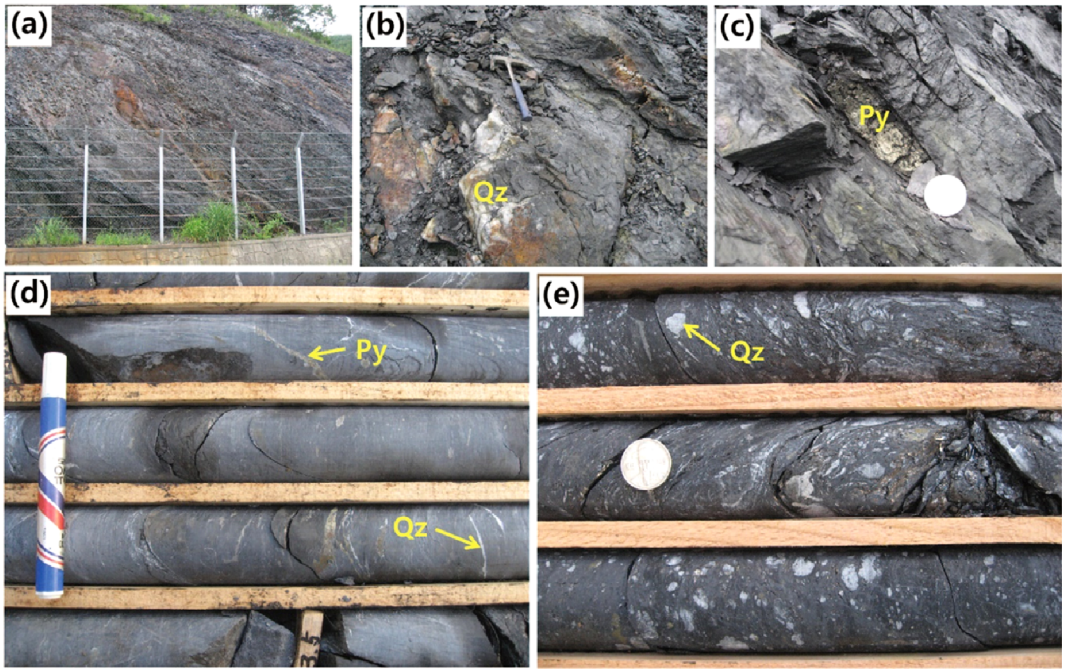

Fig. 2. Outcrop and drilled core images of the black and coaly slates in the OMB. (a) Platy and schistose black slates in Boeun, (b and c) coaly slates containing nodular quartz vein and massive sulfide minerals in Boeun, (d) black slates containing quartz and pyrite veinlets in Geumsan, and (e) coaly slates showing brecciated quartz and flow texture in Geumsan. Abbreviations: Py = pyrite, Qz = quartz.

https://doi.org/10.1007/s12303-019-0018-7

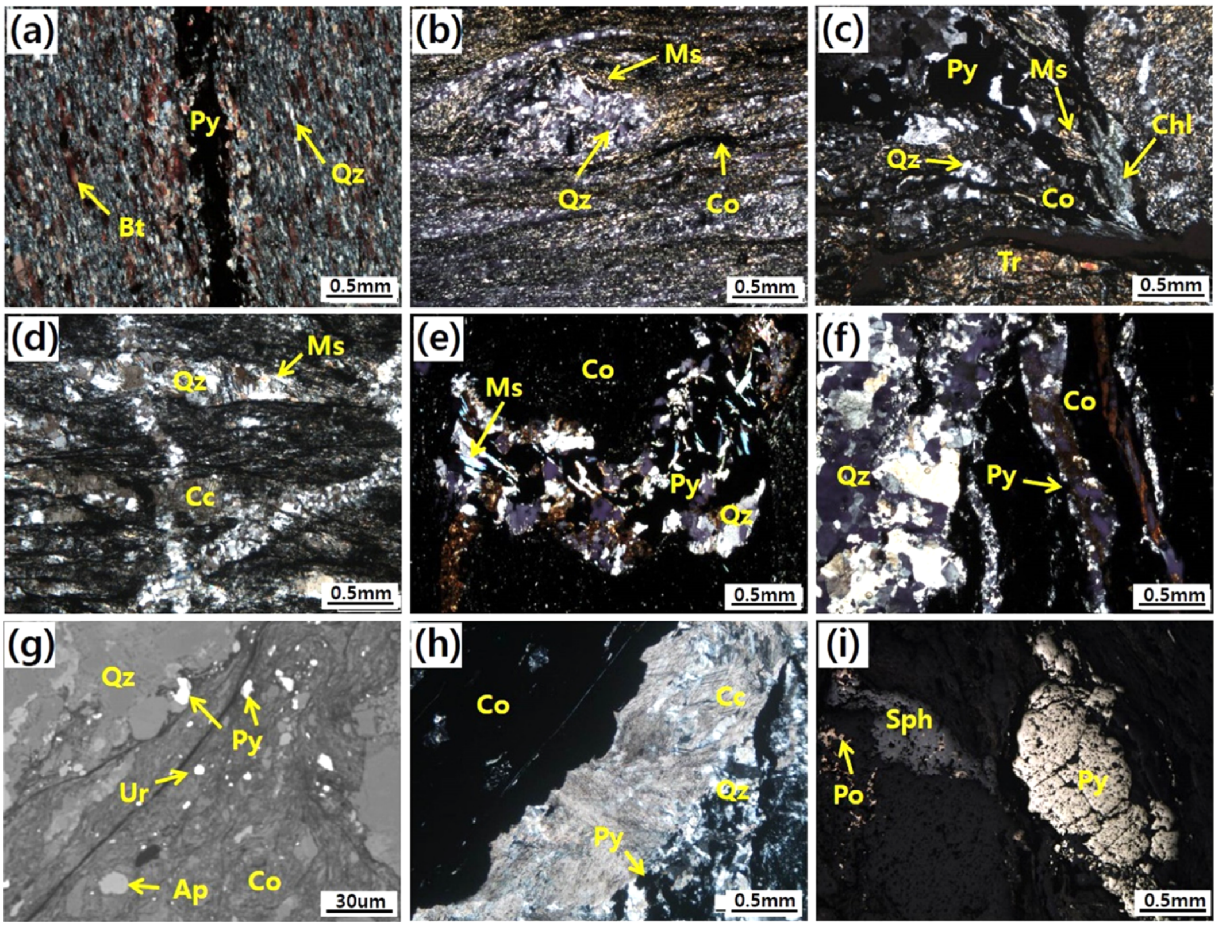

Fig. 3. Photomicrographs of black (a–d) and coaly (e–i) slates from Boeun (a and b, e and f) and Geumsan (c and d, g and i) area of the OMB. (a) Pyrite veinlet parallel to schistosity of black slate, (b) black slate showing foliated texture consisting of muscovite, quartz and coaly material, (c) black slate consisting of muscovite, chlorite, tremolite, pyrite, quartz and coal materials, (d) quartz + muscovite veinlet cutting schistosity of black slate, (e and f) coaly materials replaced by quartz + pyrite + muscovite veinlet in coaly slate, (g) BSE image of coaly slates consisting of coaly materials, quartz, pyrite, apatite and uraninite showing brecciated and flow texture, (h) quartz + calcite veinlet associated with coaly materials, and (i) pyrite, sphalerite and pyrrhotite assemblage in coaly slate. Abbreviations: Bt = biotite, Ms = muscovite, Co = coaly material, Chl = chlorite, Tr = tremolite, Cc = calcite, Ap = apatite, Ur = uraninite, Sph = sphalerite, Po = pyrrhotite. Refer to Figure 2 for others.

uranothorite, brannerite, ekanite, thorutite, and coffinite in both rock types. Of these, uraninite is the most abundant phase in the coaly slates, while uranothorite is dominant in the black slates (Shin et al., 2016).

3. METHODOLOGY

Twenty-six samples of black and coaly slates were collected at Boeun and Geumsan in the OMB (Fig. 1). The outcrops used for sampling were traced using a portable radioactivity detector and samples were also taken from a borehole comprising black and coaly slates in Geumsan area. Major elements were determined at the Korea Basic Science Institute using a Philips PW2404 X-ray fluorescence (XRF) spectrometer. Powdered samples were ignited at 950 °C and then mixed with a lithium tetraborate flux to form glass beads by fusion at 1200 °C. XRF operating conditions were a 40 kV and 30 mA current. The analytical precision was better than ±1.5%. For the analysis of trace and rare earth elements, the samples were dissolved in a mixed acid (HNO_3:HF:$HClO_4$ = 4:4:1) at 150 °C for 3 hours and then reacted with royal water + HF for additional 3 hours. After removing residual carbons by filter the samples were analyzed. Element concentrations were determined using inductively coupled plasma-atomic emission spectrometry for Sc, V, and Cr / mass spectrometry for other trace elements and REEs (ICP-AES/MS) at the Korea Basic Science Institute. The analytical precision was better than 5%. For the measurement of TOC and TS (Total sulfur), pulverized samples were subject to acid treatment with 10% HCl to remove the carbonates and then analyzed using Rock-Eval turbo 6 and LECO SC-132 analyzer at the Korea Institute of Geoscience and Mineral Resources. The analytical precision was better than 2% and 5%, respectively.

4. RESULTS

The concentrations of major and trace elements are listed in Tables 1–3. In Boeun area, the black slates have higher SiO_2 contents (avg. 61.0 wt%) but lower LOI contents (avg. 9.1 wt%) than the coaly slates which have SiO_2 contents, 54.5 wt% in average, and LOI contents, 20.5 wt% in average. Similarly, in Geumsan area, the black slates have higher SiO_2 contents (avg. 60.7 wt%) but lower LOI contents (avg. 5.6 wt%) than the coaly slates which have SiO_2 contents, 50.6 wt% in average, and LOI contents, 17.0 wt% in average. As for Al_2O_3, the coaly slates have higher contents (avg. 16.3 wt%) than the black slates (avg. 11.1 wt%) in Boeun, but they have lower contents (avg. 12.8 wt%) than the black slates (avg. 17.6 wt%) in Geumsan. Elements such as Fe_2O_3, MgO, CaO, and K_2O also show inconsistent relations between the two rock types in the study areas. Radioactivity values are consistently higher in the coaly slates (508 cpm for Boeun and 388 cpm for Geumsan in average) than in black slates (104 cpm for Boeun and 113 cpm for Geumsan in average) in both areas (Table 1).

The redox-sensitive trace elements (U, V, Mo, and Cr) in the black slates show variations from 1.4 to 11.8 ppm, 70 to 547 ppm, 0.7 to 14.7 ppm, and 64 to 194 ppm, respectively, in the study area. In the coaly slates, they vary from 9 to 370 ppm, 309 to 6957 ppm,

Table 1. Major elements concentrations (wt%) and radioactivitiy values (cpm) of the slates from the Okcheon Metamorphic Belt

Sample No.	SiO_2	Al_2O_3	TiO_2	$Fe_2O_3^{T(a)}$	MgO	MnO	CaO	Na_2O	K_2O	P_2O_5	LOI	Total	cpm
Boeun													
Black slate													
PJ-8	57.92	4.86	0.25	5.02	2.72	0.24	13.83	0.27	0.44	0.09	13.65	99.30	100
PJ-17	61.75	18.26	0.68	4.45	2.01	0.02	0.04	0.40	4.83	0.05	7.17	99.66	120
PJ-18	66.63	14.56	0.46	4.57	2.28	0.03	0.20	1.29	2.89	0.08	6.82	99.80	120
PJ-22-1	52.09	3.98	0.24	7.52	9.27	0.22	12.78	0.19	0.59	0.09	12.29	99.26	80
PJ-22-5	66.70	13.79	0.85	5.06	3.29	0.03	0.17	1.34	2.67	0.12	5.75	99.75	100
Average	61.02	11.09	0.50	5.32	3.91	0.11	5.40	0.70	2.28	0.08	9.14	99.55	104
Coaly slate													
PJ-4	50.65	14.85	0.80	4.23	1.16	0.03	0.34	0.23	4.77	0.25	22.05	99.35	400
PJ-7	49.93	16.91	0.60	0.64	1.15	0.00	0.02	0.31	5.30	0.03	24.55	99.44	520
PJ-9	56.80	16.36	0.22	0.67	0.40	0.00	0.03	0.17	1.40	0.06	24.17	100.28	540
PJ-10	56.85	18.33	0.75	3.26	1.25	0.00	0.03	0.34	4.39	0.16	14.18	99.55	600
PJ-13	58.25	15.11	0.47	2.32	1.12	0.00	0.02	0.36	4.21	0.04	17.62	99.53	480
Average	54.50	16.31	0.57	2.22	1.01	0.01	0.09	0.28	4.02	0.11	20.51	99.63	508
Geumsan													
Black slate													
BS-6	62.73	17.56	0.66	4.76	2.48	0.06	0.08	1.08	4.20	0.05	6.50	100.16	75
BS-7	58.68	18.94	0.74	6.03	3.24	0.10	0.49	0.83	4.20	0.35	6.25	99.86	110
BS-8	59.80	18.75	0.80	6.16	3.03	0.14	0.09	2.02	4.12	0.05	4.12	99.08	120
BS-9	50.87	18.46	0.72	7.88	4.43	0.14	2.52	0.90	3.54	1.87	8.09	99.42	110
BS-10	71.48	12.16	0.48	6.53	1.79	0.06	0.13	0.45	2.82	0.03	3.51	99.46	105
BS-11	60.35	18.44	0.66	6.35	3.00	0.10	0.09	1.04	4.09	0.05	5.33	99.51	120
BS-12	65.40	15.67	0.58	6.24	2.45	0.08	0.09	1.57	3.58	0.04	5.20	100.90	95
BS-13	57.11	19.60	0.79	6.90	2.81	0.10	0.12	0.83	4.81	0.05	6.18	99.30	150
BS-14	59.99	18.62	0.69	6.32	2.56	0.09	0.30	1.06	4.67	0.05	5.62	99.98	135
Average	60.71	17.58	0.68	6.35	2.87	0.10	0.44	1.09	4.00	0.28	5.64	99.74	113
Coaly slate													
BS-15	55.17	14.59	0.53	6.99	3.59	0.02	1.41	0.45	4.59	0.20	11.75	99.31	360
BS-16	48.95	9.23	0.44	8.64	4.99	0.02	2.26	0.05	2.30	0.56	21.62	99.07	660
BS-17	47.27	13.13	0.55	8.62	4.49	0.03	2.41	0.35	3.21	0.36	19.90	100.32	320
BS-18	47.24	12.87	0.54	7.46	3.49	0.05	4.66	0.49	3.31	0.40	19.12	99.64	450
BS-19	45.91	12.73	0.48	7.23	3.19	0.04	3.80	1.08	3.36	0.38	21.06	99.26	460
BS-20	59.22	14.47	0.52	6.07	2.54	0.04	3.16	4.03	1.72	0.08	8.37	100.22	80
Average	50.63	12.84	0.51	7.50	3.71	0.03	2.95	1.08	3.08	0.33	16.97	99.64	388

[(a)] $Fe_2O_3^T$ is total iron as Fe_2O_3; LOI is loss on ignition; cpm = counts per minutes.

https://doi.org/10.1007/s12303-019-0018-7

Table 2. Concentrations of redox-sensitive trace elements and rare earth elements (ppm) in the slates from Boeun area

Rock type	Black slate					Average	Coaly slate				
Sample No.	PJ-8	PJ-17	PJ-18	PJ-22-1	PJ-22-5		PJ-4	PJ-7	PJ-9	PJ-10	PJ-13
Sc	< 10	14.7	15.5	15.2	14.5	13.0	3.2	19.3	< 10	16.0	17.0
V	88.1	547.1	274.4	70.0	88.7	213.7	6957.0	3564.0	3092.0	3454.0	1149.0
Cr	101.4	115.7	124.4	63.6	127.1	106.4	349.7	242.7	296.4	264.0	177.7
Co	5.7	32.3	8.5	23.6	23.7	18.8	16.8	1.6	0.5	1.4	1.6
Ni	24.8	90.2	41.6	84.1	81.3	64.4	339.7	12.3	6.5	24.9	10.5
Mo	1.6	6.8	14.7	0.7	0.9	4.9	262.0	69.3	133.2	279.5	78.4
Th	5.1	9.5	9.4	4.2	7.0	7.1	8.7	6.0	5.8	14.4	6.1
U	1.6	11.8	10.7	1.4	2.1	5.5	72.4	9.0	60.2	123.3	6.8
S_{tot} (wt%)	0.71	0.75	0.47	8.47	2.52	2.58	1.18	0.13	0.04	0.02	0.08
TOC (wt%)	11.6	8.7	3.2	1.2	0.9	5.1	10.4	10.4	7.7	5.9	10.6
La	12.08	32.64	39.03	10.21	22.63	23.32	35.34	57.97	17.11	42.45	36.33
Ce	24.03	58.93	71.98	20.96	52.37	45.65	58.67	84.26	25.58	74.71	53.34
Pr	2.66	7.50	8.56	2.34	5.49	5.31	8.07	13.18	3.66	9.71	8.84
Nd	14.39	37.48	44.31	12.64	29.87	27.74	40.36	63.70	18.11	48.77	41.99
Sm	2.34	5.15	5.80	2.46	4.07	3.96	5.85	10.88	5.96	14.36	11.00
Eu	0.60	1.42	1.47	0.70	0.95	1.03	2.71	5.15	3.00	7.34	4.65
Gd	2.21	4.89	5.82	2.23	4.44	3.92	6.94	10.58	2.65	5.91	7.16
Tb	0.25	0.61	0.68	0.25	0.56	0.47	0.95	1.38	0.29	0.72	0.94
Dy	1.80	4.06	4.09	1.76	3.42	3.03	6.58	8.92	2.19	4.77	6.26
Ho	0.34	0.80	0.77	0.32	0.63	0.57	1.47	1.93	0.45	0.99	1.33
Er	1.21	2.67	2.52	1.12	2.02	1.91	4.75	6.26	1.55	3.29	4.32
Tm	0.14	0.34	0.31	0.13	0.25	0.23	0.63	0.83	0.17	0.41	0.58
Yb	1.25	2.59	2.31	1.17	2.00	1.86	4.29	5.73	1.32	2.90	4.00
Lu	0.17	0.35	0.32	0.16	0.27	0.25	0.61	0.83	0.23	0.46	0.60
La_N/Yb_N	0.97	1.26	1.69	0.87	1.13	1.19	0.82	1.01	1.30	1.47	0.91
Ce/Ce*	0.86	0.79	0.81	0.87	0.96	0.86	0.73	0.65	0.67	0.77	0.64
Eu/Eu*	1.33	1.39	1.28	1.50	1.13	1.33	2.11	2.34	3.08	3.11	2.33
SUM(REE)	63.5	159.4	188.0	56.5	129.0	119.3	177.2	271.6	82.3	216.8	181.3

Half values were used for calculations of averages for samples with values below detection limit.

13.8 to 279 ppm, and 158 to 476 ppm, respectively. In both areas, these elements show much higher concentrations in the coaly slates than in the black slates. The REE abundances in the black slates and the coaly slates are presented in Tables 2 and 3. The concentrations range from 56 to 188 ppm (avg. 119 ppm) for the black slates and from 82 to 272 ppm (avg. 186 ppm) for the coaly slates in Boeun. They range from 106 to 243 ppm (avg. 175 ppm) for the black slates and from 154 to 230 ppm (avg. 191 ppm) for the coaly slates in Geumsan. In both areas, the REE concentrations are higher in the coaly slates than those in the black slates, though the difference is not so significant in Geumsan.

The REEs and trace element concentrations were normalized to the North American Shale Composite (NASC) reference standard (Figs. 4 and 5) provided by Gromet et al. (1984), and by Degens et al. (1958) and Wedepohl (1974), for V and Mo, respectively. The Eu anomaly ($Eu^* = 3Eu_N/(2Sm_N + Tb_N)$) and Ce anomaly ($Ce^* = 3Ce_N/(2La_N + Nd_N)$) were calculated to evaluate the redox-condition and genetic environment. The Eu anomaly values range from 1.1 to 1.5 (avg. 1.3) for the black slates and from 2.1 to 3.1 (avg. 2.6) for the coaly slates in Boeun, and from 0.9 to 1.0 (avg. 0.9) for the black slates and from 1.1 to 2.4 (avg. 1.6) for the coaly slates in Geumsan. The Ce anomaly values vary from 0.79 to 0.96 (avg. 0.86) for the black slates and 0.64 to 0.77 (avg. 0.69) for the coaly slates in Boeun, and they range from 0.82 to 0.87 (avg. 0.84) for the black slates and 0.71 to 0.83 (avg. 0.76) for the coaly slates in Geumsan. Though the values of La_N/Yb_N for the black slates (avg. 1.13) and coaly slates (avg. 1.10) from Boeun are slightly higher than those from Geumsan (avg. 1.00 and 1.03, respectively), the differences between the two rock types in each area are relatively small.

The TOC abundances are also listed in Tables 2 and 3. They vary from 0.9 to 11.6 wt% (avg. 5.1 wt%) in the black slates and from 5.9 to 10.6 wt% (avg. 9.0 wt%) in the coaly slates from Boeun. They range from 0.7 to 3.7 wt% (avg. 1.9 wt%) in the black slates

Table 3. Concentrations of redox-sensitive trace elements and rare earth elements (ppm) in the slates from Geumsan area

Rock type	Black slate									Average	Coaly slate						Average
Sample No.	BS-6	BS-7	BS-8	BS-9	BS-10	BS-11	BS-12	BS-13	BS-14		BS-15	BS-16	BS-17	BS-18	BS-19	BS-20	
Sc	18.8	22.2	18.9	21.7	12.7	18.6	16.5	18.5	18.2	18.4	14.5	10.9	14.2	13.3	13.8	12.4	13.2
V	467.3	231.3	119.5	194.8	182.5	182.3	198.9	213.6	237.3	225.3	970.3	3011.5	1881.7	2645.2	3082.8	309.4	1983.5
Cr	194.0	106.7	105.1	114.5	148.1	100.9	94.5	104.7	114.7	120.4	476.7	435.2	234.5	254.2	452.2	158.3	335.2
Co	9.3	10.4	11.1	13.3	29.5	13.9	15.3	13.5	14.0	14.5	16.2	24.2	26.7	22.5	22.1	17.9	21.6
Ni	52.2	38.7	23.0	47.6	85.1	55.3	55.6	42.5	48.8	49.9	55.4	42.3	48.6	37.7	43.8	70.8	49.7
Mo	12.8	5.3	1.2	4.8	6.7	4.1	6.6	4.8	5.6	5.8	103.4	357.9	194.3	231.7	148.3	13.8	174.9
Th	19.0	17.1	18.3	17.8	12.3	16.8	14.6	19.2	19.3	17.2	15.0	11.6	14.9	14.5	14.0	15.5	14.3
U	9.5	5.6	3.2	6.5	4.0	5.0	8.1	5.4	5.6	5.9	86.6	370.1	177.0	226.9	206.8	12.1	179.9
S_{tot} (wt%)	0.71	0.87	0.46	0.85	1.69	1.16	1.47	1.12	1.47	1.09	1.57	2.41	2.63	2.39	2.44	1.13	2.10
TOC (wt%)	3.0	2.3	0.7	3.7	0.9	1.4	1.8	1.7	1.7	1.9	6.5	12.8	21.7	10.2	14.5	13.3	13.2
La	35.80	31.77	36.15	42.89	20.78	31.24	26.75	38.60	39.46	33.72	34.04	33.51	42.03	46.08	42.98	31.37	38.34
Ce	67.39	61.17	71.73	82.86	39.96	60.93	51.60	75.24	76.24	65.24	61.90	53.47	72.35	76.72	69.72	58.97	65.52
Pr	8.26	7.23	8.13	10.01	4.73	7.13	6.16	8.78	9.15	7.73	7.66	7.24	9.40	10.25	9.60	7.00	8.53
Nd	41.34	37.03	41.78	51.46	23.79	36.08	30.98	44.44	46.01	39.21	38.59	36.43	47.11	50.82	47.46	35.33	42.62
Sm	6.08	5.79	5.55	9.13	3.36	5.21	4.46	6.24	6.60	5.82	6.01	6.33	7.69	8.39	8.09	5.16	6.95
Eu	1.27	1.17	1.12	1.86	0.71	1.08	0.93	1.25	1.27	1.18	1.40	3.44	2.77	3.35	2.03	1.54	2.42
Gd	5.89	5.86	5.27	10.44	3.49	5.64	4.41	6.62	6.26	5.99	5.93	7.81	8.59	9.34	8.80	4.68	7.53
Tb	0.84	0.88	0.77	1.69	0.54	0.90	0.68	1.05	0.89	0.92	0.83	1.16	1.25	1.38	1.27	0.62	1.09
Dy	5.07	5.44	4.58	11.36	3.44	5.88	4.26	6.63	5.23	5.77	5.03	7.48	7.89	8.67	8.07	3.46	6.77
Ho	1.07	1.15	0.96	2.54	0.73	1.26	0.91	1.41	1.07	1.23	1.08	1.75	1.75	1.95	1.83	0.69	1.51
Er	3.30	3.54	2.94	8.16	2.22	3.83	2.82	4.27	3.24	3.81	3.29	5.29	5.35	5.96	5.67	2.07	4.61
Tm	0.48	0.53	0.43	1.24	0.32	0.55	0.41	0.61	0.47	0.56	0.46	0.73	0.74	0.83	0.77	0.31	0.64
Yb	3.18	3.51	2.87	8.07	2.08	3.47	2.67	3.88	3.03	3.64	2.97	4.41	4.55	5.07	4.76	2.02	3.96
Lu	0.49	0.53	0.43	1.15	0.31	0.51	0.40	0.57	0.45	0.54	0.45	0.64	0.67	0.75	0.71	0.31	0.59
La_N/Yb_N	1.13	0.91	1.26	0.53	1.00	0.90	1.00	1.00	1.30	1.00	1.15	0.76	0.92	0.91	0.90	1.55	1.03
Ce/Ce*	0.82	0.84	0.87	0.83	0.84	0.85	0.84	0.85	0.84	0.84	0.80	0.71	0.76	0.74	0.72	0.83	0.76
Eu/Eu*	1.01	0.94	0.97	0.88	0.97	0.92	0.97	0.90	0.93	0.94	1.12	2.37	1.64	1.81	1.16	1.50	1.60
SUM(REE)	180.5	165.6	182.7	242.9	106.5	163.7	137.4	199.6	199.4	175.4	169.6	169.7	212.1	229.6	211.8	153.5	191.1

and from 6.5 to 21.7 wt% (avg. 13.2 wt%) in the coaly slates from Geumsan. Total sulfur contents vary from 0.71 to 8.47 wt% (avg. 2.58 wt%) in the black slates and from 0.02 to 1.18 wt% (avg. 0.29 wt%) in the coaly slates from Boeun. They range from 0.46 to 1.69 wt% (avg. 1.09 wt%) in the black slates and from 1.13 to 2.63 wt% (avg. 2.1 wt%) in the coaly slates from Geumsan.

5. DISCUSSION

5.1. Geochemistry of Redox-sensitive Trace Elements

The concentrations of the redox-sensitive elements such as V, Mo, Cr, Mn, U, and Th in black shales have been utilized for evaluating the depositional conditions of the sediments (Arthur and Sageman, 1994; Morford and Emerson, 1999; Fleurance et al., 2013). Our data show that V, Cr, Mo, and U are highly enriched from a few times up to hundreds of times in the coaly slates relative to the NASC standard, while Mn, Co, and Ni show depletion in the coaly slates, and the others do not show particular differences (Fig. 5). On the contrary, much less enrichments or depletions for those elements are noticed in the samples of the black slates.

The enrichment of the redox-sensitive elements has been generally considered as strong evidences for anoxic conditions in the depositional environment (Algeo and Maynard, 2004; Pi et al., 2013). Particularly, V is significantly enriched as a result of accumulating in anaerobic environment after existing as an ion state in an oxidizing environment (Francois, 1988). In oxic environments, V is present as V^{5+}, and under more reducing conditions, it is reduced to V^{4+}, and further to V^{3+}, which can be precipitated as V_2O_3 (Tribovillard et al., 2006). It may be supported by the occurrence of vanadium-muscovite in the coal formation of the OMB, in which V possibly substituted octahedral Al of muscovite (Lee and Lee, 1997).

It has been known that under oxic conditions, Mo is present as Mo^{4+} in seawater, but it may be reduced to MoS_4^{2-} in more reducing environment under organic-rich sediment (Algeo and

https://doi.org/10.1007/s12303-019-0018-7

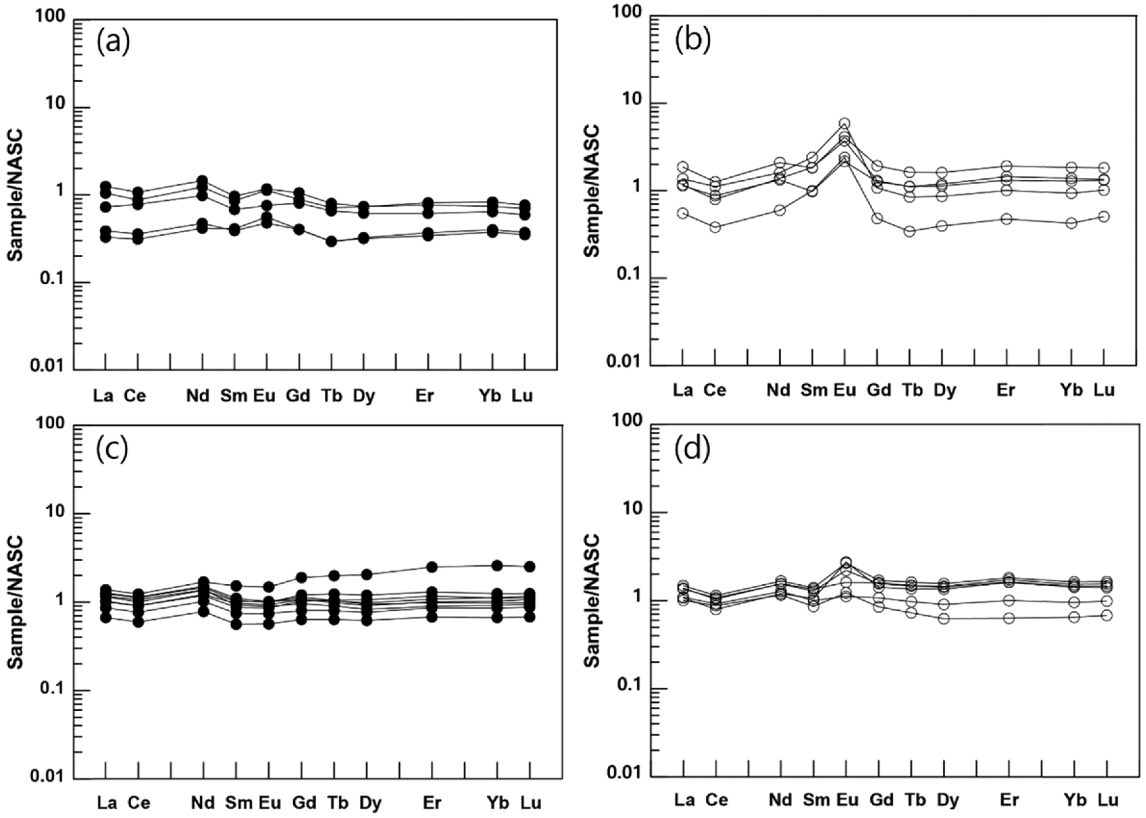

Fig. 4. REE patterns normalized by NASC for the black slates (solid circle) and coaly slates (open circle) from Boeun (a and b) and Geumsan (c and d) in the OMB.

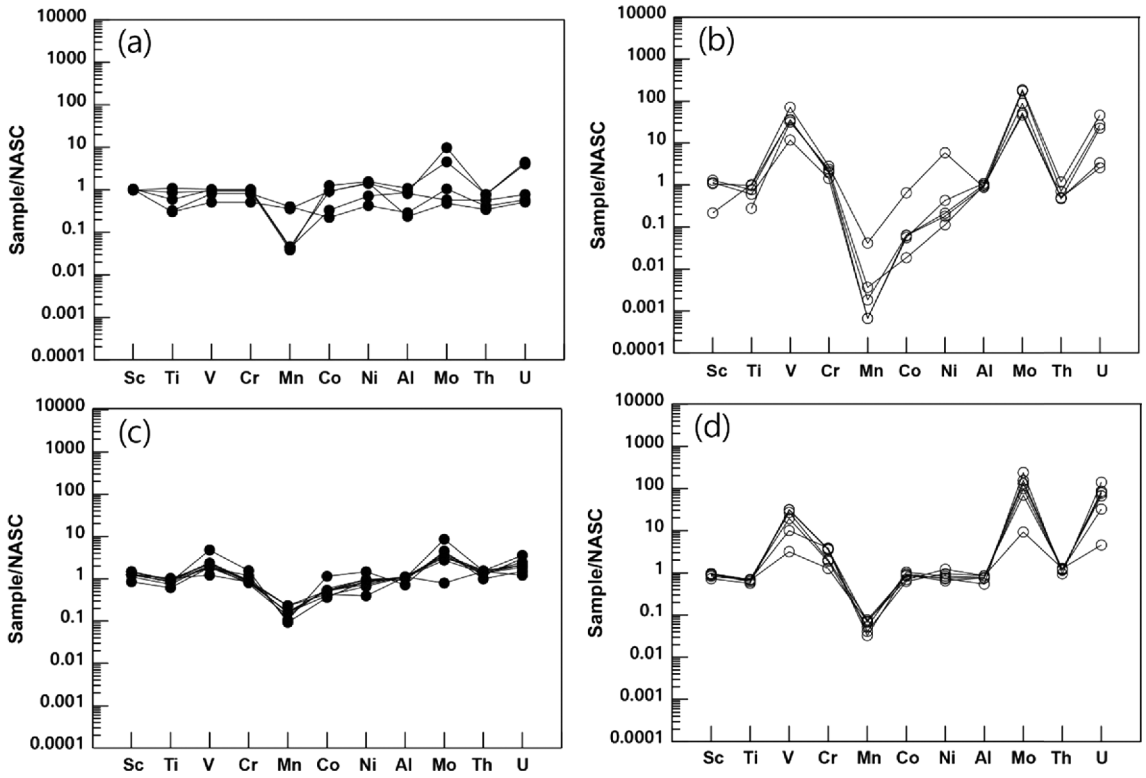

Fig. 5. Concentrations of some redox-sensitive elements (V, Cr, Mn, Co, Ni, Mo, Th, U), as well as Sc, Ti and Al for the black slates (solid circle) and coaly slates (open circle) from Boeun (a and b) and Geumsan (c and d) in the OMB. The values were normalized to NASC (Gromet et al., 1984), except V (Degens et al., 1958) and Mo (Wedepohl, 1974).

Maynard, 2004). It was documented that tiny (1–2 μm) molybdenite (MoS_2) flakes are commonly scattered in the fine-grained coaly matrix in the OMB (Jeong and Lee, 2001). As indicated by general association of metal enrichment with organic-rich sediments under anoxic conditions, common occurrences of molybdenite indicate more reducing depositional conditions of the coaly slates in the OMB. In this study, Mo contents are also broadly correlated with V contents, and the coaly slates exhibit higher Mo and V contents than those of the black slates (Tables 2 and 3), which again indicates that the coaly slates may have been deposited under more reducing conditions (anoxic-euxinic) than those of the black slates.

Similarly to V and Mo, in an oxic environment, Cr may exist as Cr^{4+}, but, under anoxic conditions, it is reduced to Cr^{3+} which can be precipitated as insoluble $Cr(OH)_3$ or Cr_2O_3 in sediments (Algeo and Maynard, 2004). Thus, consistent higher Cr concentrations up to 477 ppm in the coaly slates indicate more reducing depositional conditions in the OMB.

Under oxic conditions, Mn is mainly present as Mn^{3+} or Mn^{4+} hydroxides or oxides (e.g., MnO_2) that are highly insoluble, but under reducing conditions, it is reduced to Mn^{2+}. It was also documented that the solubility of Mn^{2+} in sediments is enhanced under reducing conditions, thus, leading to a depletion of Mn in the sediments (Hild and Brumsack, 1998). Quinby-Hunt and Wilde (1994) proposed four groups of redox conditions based on the Mn contents in black shales. In group 1 (oxic), Mn occurs as Mn(III, IV) oxides and appears in relatively high concentrations (avg. 1,300 ppm). In group 2 (anoxic), Mn is reduced to Mn^{2+} as is evidenced by low Mn concentration (avg. 310 ppm). In group 3, Mn is reduced and relatively soluble reflecting anoxic conditions, with lower Mn concentration (avg. 170 ppm). Group 4 black shales deposited under environmental conditions favoring high organic preservation have Mn concentration less than 260 ppm with 80 ppm average.

According to the classification, the coaly slates in the OMB seem to have been deposited under anoxic to reducing conditions, as indicated by low Mn concentrations of 45 ppm on average in Boeun and 266 ppm on average in Geumsan (Table 1). Mn could be supplied by hydrothermal venting in submarine environment (Klinkhammer et al., 1983), which is associated with the formation of the metalliferous black slates in the OMB (Jeong, 2006; Shin et al., 2016). However, the analyzed samples in this study were depleted relative to the NASC standard for this element. Thus, the lower Mn concentrations may indicate that the coaly slates formed in an environment in which anoxic conditions favored the reduction to the more soluble Mn^{2+}.

The relationship between TOC and trace elements has been utilized to interpret the depositional environments of metalliferous black shales (Algeo and Maynard, 2004; Slack et al., 2004). Under oxic to suboxic marine conditions, U exists as soluble U^{6+}, but in reducing conditions, it is reduced to U^{4+} to form uraninite crystals (Anderson et al., 1989). The decrease in U^{6+} is mostly related to the reduction in sulfides by bacteria, and this decrease is closely related to the amount of organic matter (Tribovillard et al., 2006). It has been noted that uraninite is much more abundant in the coaly slates than the black slates (Shin et al., 2016). Thus, the general tendency of a positive correlation between TOC and U as a group for the black and coaly slates from Boeun and Geumsan,

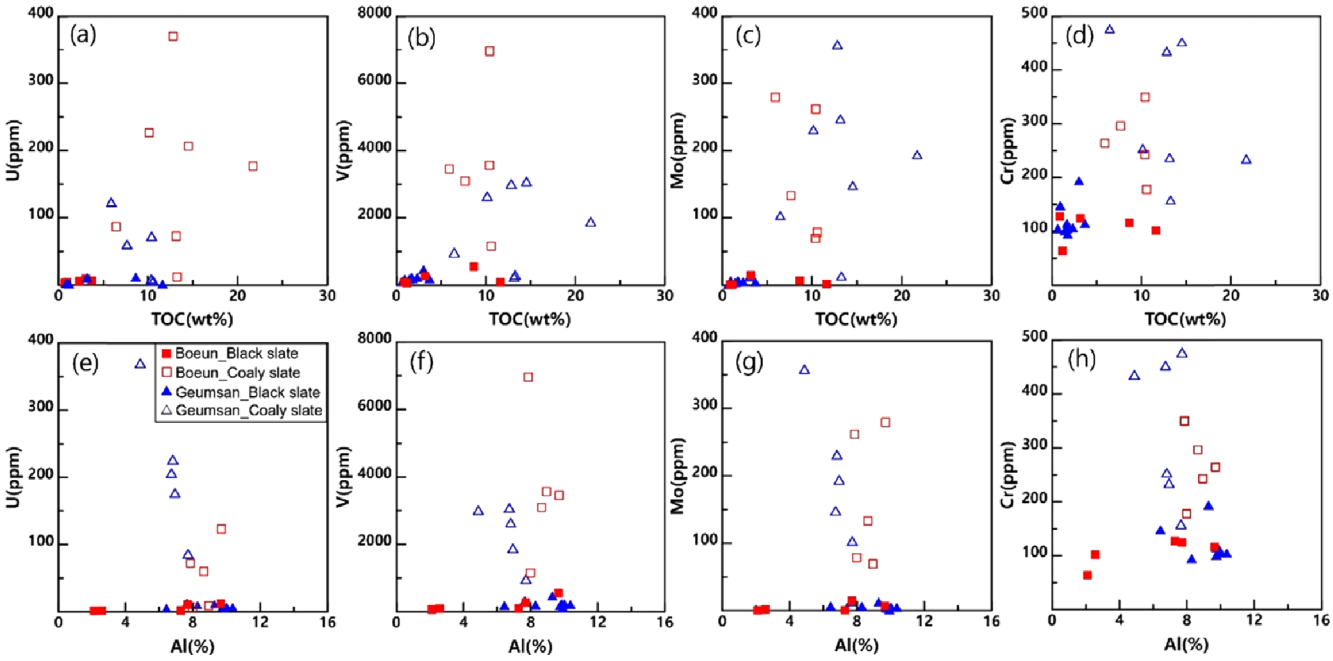

Fig. 6. Plots of metal contents against TOC and Al contents in the black and coaly slates of the OMB.

https://doi.org/10.1007/s12303-019-0018-7

respectively, indicate the crucial effect of U reduction related to organic matter. In our study, V, Cr, and Mo also show a moderate tendency of positive correlation with TOC, though the relationship seems to be better established for the samples from Geumsan than Boeun (Figs. 6a–d).

Element ratios of redox sensitive elements have also been utilized for evaluating the depositional conditions of the sediments. Higher V/(V + Ni) and V/Cr ratios indicate more strongly reducing conditions (Hatch and Leventhal, 1992; Jones and Manning, 1994; Zhou and Jiang, 2009) as, under anoxic condition, V tends to accumulate more significantly in sediments than other elements. In our study, V/(V + Ni) ratios were 0.70–0.81 for the black slates and 0.95–0.99 for the coaly slates. The ratios of V/Cr were 1.85–1.92 for the black slates and 6.03–9.39 for the coaly slates. In addition, Ni/Co ratios are much higher in coaly slates, 11.35–48.78, than black slates, 3.07–3.80 (Table 4). Both of these results indicate that the redox conditions for the formation of the coaly slates were more reducing (anoxic-euxinic) than those for the black slates.

The usefulness of the U/Th ratios as an indicator of relatively oxidizing or reducing conditions has been demonstrated (Jones and Manning, 1994; Zhao et al., 2016). Th is unaffected by redox conditions and exists as insoluble Th^{4+}. On the contrary, U is present as either insoluble U^{4+} or soluble U^{6+}, leading to uranium enrichment or depletion in sediments under highly reducing conditions and oxidizing conditions, respectively. Thus, the U/Th ratios and ΔU, defined as ΔU = U/(0.5*(U + Th/3), could be used as a proxy for redox conditions of the depositional environment with values > 1.25 and > 1 for anoxic environments and values < 0.75 and < 1 for oxidizing environments, respectively (Jones and Manning, 1994; Wignall, 1994). Fairly high values, 5.98–13.45 for U/Th and 1.79–1.86 for ΔU, of the coaly slates indicate a reducing environment, commonly marine (Carvalho et al., 2011), while lower values, < 0.66 and < 1.20, respectively, for the black slates are associated with U mobilization through weathering and/or leaching, and therefore indicate an oxidizing, possibly nearshore/terrestrial environment.

In general, marine samples tend to be enriched with heavy REEs and to show a Ce deficiency compared to that of La, Pr, or Nd, which is known to be a major feature of marine shales (Elderfield and Greaves, 1982; Sotto and Yoshiyuki, 1999). A positive Ce anomaly can be established as a result of the precipitation of a CeO_2 form into sediments when the soluble Ce^{3+} in seawater is oxidized to the insoluble Ce^{4+}, and thus it can be used to trace redox conditions in paleo-ocean bottom waters (German and Elderfield, 1990; Shields and Stille, 2001; Pattan et al., 2005). In this study, both rock types show negative Ce-anomalies, 0.69 and 0.76 for the coaly slates and 0.86 and 0.84 for the black slates in Boeun and Geumsan, respectively. Accordingly, the coaly slates with lower Ce/Ce* values could reflect more reducing conditions than the black slates during their formation.

5.2. Influence of Hydrothermal Fluid Activity

The most prominent feature in the comparison of REE variations between the black slates and the coaly slates in the study area was the enrichment of REE concentration and the positive Eu anomalies (Eu/Eu* as high as 3.1) in the coaly slate (Fig. 4). It has been reported that Eu enrichment appears to be prominent in present-day submarine hydrothermal activities (Craddock, 2010), but depleted in hydrothermal systems related to continental settings (Michard and Albarede, 1986). This is due to the fact that the mobility of Eu is greatly influenced by redox and temperature conditions. Eu is characterized by enrichment under a high temperature (> 250 °C) reducing environment, but by depletion in a low temperature oxidizing environment (Michard et al., 1983; Parr, 1992).

It also has been reported that negative Eu anomalies in chondrite-normalized REE patterns for black shales indicate deposition from fluids with a temperature < 200 °C (Young et al., 2013) due to the inert nature of Eu^{3+} under normal temperature conditions. Meanwhile, in case of extreme reducing and alkaline conditions, a reduction of Eu^{3+} to divalent form of Eu is common (Steiner et al., 2001). Thus, it can be interpreted that the positive Eu anomalies of the coaly slate in the study area were affected by hydrothermal activity under a high temperature reducing condition on the seafloor.

According to Bostrom (1983), U/Th ratios reflect the depositional condition of sedimentary rocks and normal sedimentary rocks have U/Th values less than 1. However, when hydrothermal

Table 4. Redox-sensitive trace element ratios for various depositional environments

Sedimentary environment Indicators	Anoxic	Suboxic	Oxic	Boeun		Geumsan		References
				Black slate	Coaly slate	Black slate	Coaly slate	
V/(V + Ni)	> 0.60	0.46–0.60	< 0.46	0.70	0.99	0.81	0.95	Hatch and Leventhal (1992)
V/Cr	> 4.25	2.00–4.25	< 2.00	1.92	9.39	1.85	6.03	Jones and Manning (1994)
Ni/Co	> 7.00	5.00–7.00	< 5.00	3.80	11.35	3.07	48.78	Jones and Manning (1994)
U/Th	> 1.25	0.75–1.25	< 0.75	0.66	5.98	0.35	13.45	Jones and Manning (1994)
ΔU[(a)]	> 1		< 1	1.20	1.79	0.99	1.86	Wignall (1994)

[(a)] ΔU = U/(0.5*(U + Th/3)).

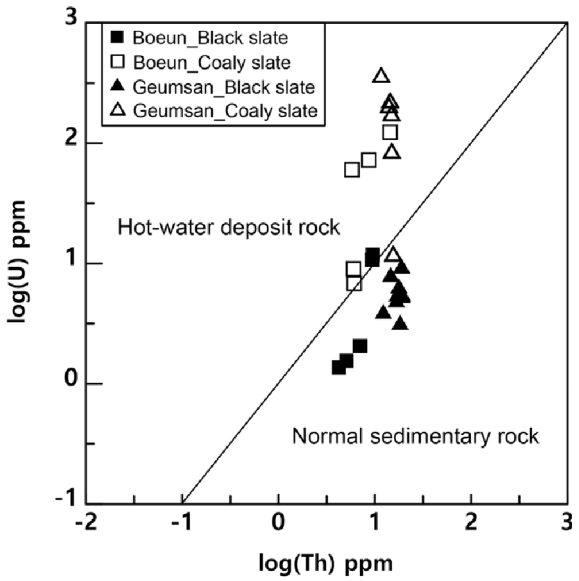

Fig. 7. U-Th correlation diagram for the black and coaly slates in the OMB (according to Bostrom, 1983).

system prevails, the values are above 1. In the case of the black slates in this study, the U/Th ratios are mostly less than 1, while most of the coaly slates are plotted above 1 (Fig. 7). The results also corroborate the interpretation that U enrichment in the coaly slates was influenced by hydrothermal activities. Thus, general positive relationships of U/Th and ΔU with TOC concentration (Fig. 8) might reflect the effects of hydrothermal fluids to not only the enrichment of organic matter but also its preservation.

5.3. Genetic Implication and Comparison with Metalliferous Black Shales in South China

The OMB has been regarded as the northeastern extension of the Early Cambrian basin of the South China Block (Chang, 1996; Ree et al., 2001; Choi et al., 2012; Chough, 2013) (Fig. 1). Based on the similarities of mineralogy, geochemistry, and petrographic characteristics, the metalliferous black slates in the OMB were also considered as a metamorphic analogue of the black shales in the South China Block (Jeong, 2006; Shin et al., 2016). Thus, the comparison of metal enrichment process between the OMB and the South China Block would further

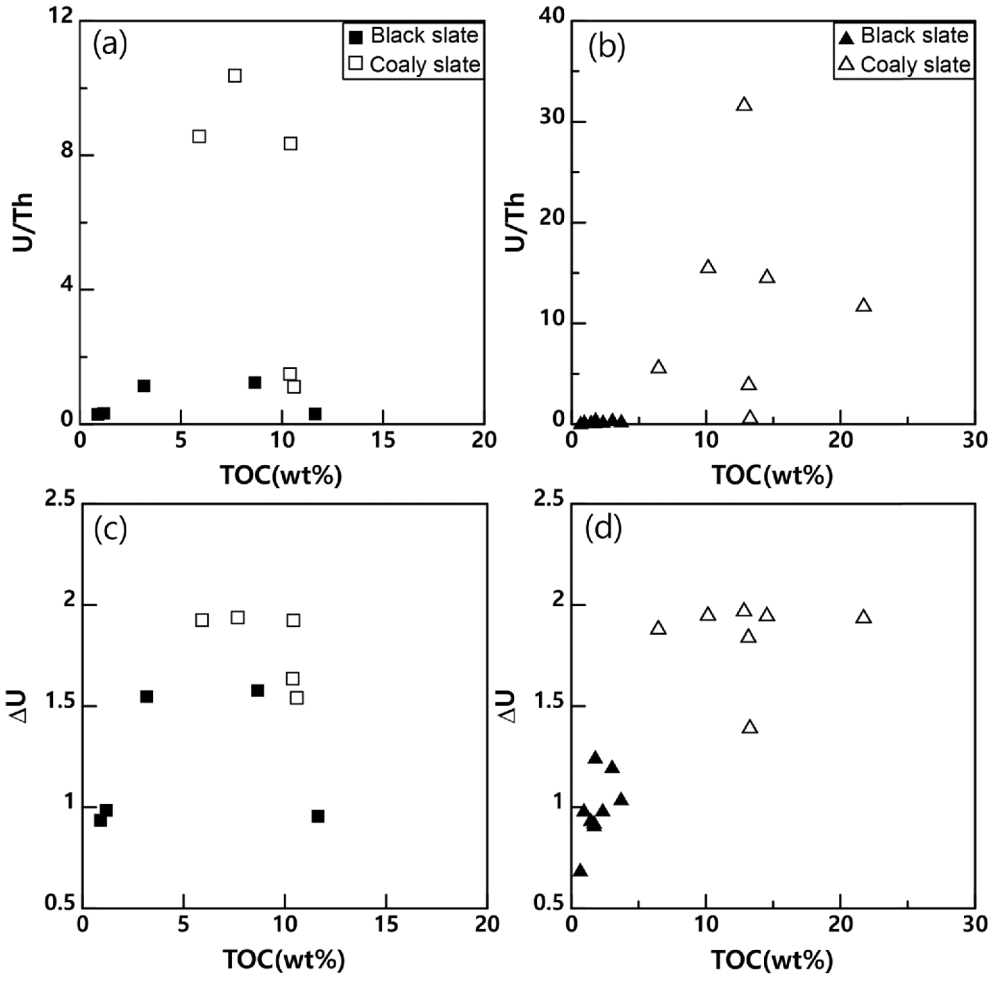

Fig. 8. Plots of U-Th ratios against TOC contents in the black and coaly slates from Boeun (a and c) and Geumsan (b and d) in the OMB.

https://doi.org/10.1007/s12303-019-0018-7

help understand the evolution history of each tectonic province. Metalliferous black shales in South China have drawn much attention for their genetic implications as well as potential metallic ore deposits (Lott et al., 1999; Steiner et al., 2001; Mao et al., 2002; Coveney, 2003; Jiang et al., 2006; Pasava et al., 2008; Xu et al., 2013; Lehmann et al., 2016). The black shales are locally interbedded with, several centimeter-thick, polymetallic Ni-Mo-PGE-Au sulfide ore layers with additional trace metals such as Zn, Cu, Pb, V, and U in the sequence of the Niutitang Formation, and they extend for about 1,600 km on the Yangtze Platform (Mao et al., 2002).

However, there still has been much controversy over the causes of metal enrichment either by seawater or hydrothermal origin, or by multiple sources. It has been argued that restricted and lenticular occurrences, extreme variable thickness, wide range of hydrothermal brine salinities, and turbiditic textures of ore bodies are the results of submarine hydrothermal venting process on the seafloor, which was regarded as sedimentary exhalative process (Lott et al., 1999; Steiner et al., 2001; Coveney, 2003; Jiang et al., 2006, 2009). In contrast, Mao et al. (2002) and Lehmann et al. (2007) insisted that the ore constituents were enriched by scavenging process in seawater at a very low sedimentation rate. Based on Mo and Cr isotopes as well as trace element geochemistry, it was further interpreted as a combination of redox cycling and interface scavenging at bottom under euxinic conditions, and of oxidation of organic matter settling from the photic zone (Xu et al., 2013; Lehmann et al., 2016). On the other hand, Pasava et al. (2008) argued that, though Mo could be derived from normal seawater, much higher Ni concentrations could hardly be originated from a single source of average seawater. They interpreted that hydrothermal brines might have leached metals from footwall sequences and became, after mixing with normal seawater, an additional source of Ag, Cr, Cu, Pb, Sb, Zn, Ni, PGE, V and other metals for the deposits.

The metal enrichment processes of the metalliferous black slates in the OMB are also discussed as follows. To evaluate the effect of detrital input for the black slates and the coaly slates in the OMB, plots of Al versus U, V, Mo, and Cr are constructed (Figs. 6e–h). Aluminum is commonly of detrital origin in black shales and tends to establish good positive correlations with accompanied elements (Algeo and Maynard, 2004). However, no systematic correlations are observed between the two rock types, suggesting that the metals were unlikely to be of detrital origin. In addition, despite the different concentration patterns of some major elements (e.g., TiO_2, Fe_2O_3, MgO, CaO) between the two study areas, consistently lower SiO_2 but higher TOC contents in the coaly slates and variable Al_2O_3 contents in study areas also support the idea that simple hydrothermal remobilization or alteration of preexisting black slates were not crucial in the metal enrichments in the OMB. On the other hand, general positive correlations for the black slates and the coaly slates as a group between TOC and the metals indicate the possible contribution of organic matters for the enrichment (Figs. 6a–d). (e.g., Mao et al., 2002; Kunzmann et al., 2015; Baioumy and Lehmann, 2017).

However, the strong metal enrichments in the coaly slates seem to have been influenced not only by a simple precipitation in normal seawater with organic-rich sediment, but also by submarine hydrothermal activities (e.g., Steiner et al., 2001; Pasava et al., 2008; Pi et al., 2014). The typical Eu enrichments and the prominence of negative Ce anomalies in the coaly slates as manifested in the negative correlation between the Ce and Eu anomalies (Fig. 9) indicate that the REE mobilization was strong during the formation of the coaly slates under the influence of submarine hydrothermal activities and shale deposition. In

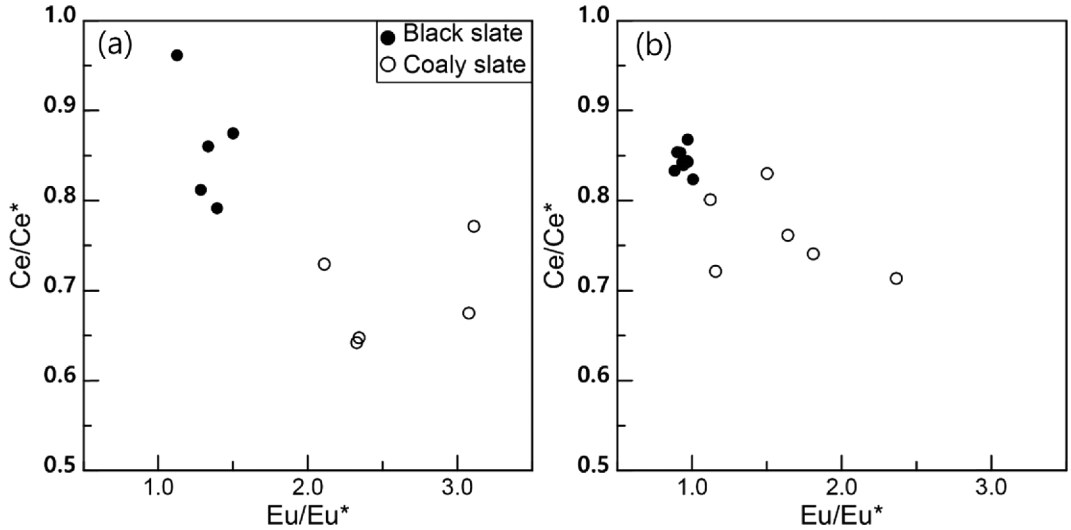

Fig. 9. Plots of Ce versus Eu anomaly ratios calculated from the NASC-normalized REE abundances for the black and coaly slates from Boeun (a) and Geumsan (b) in the OMB.

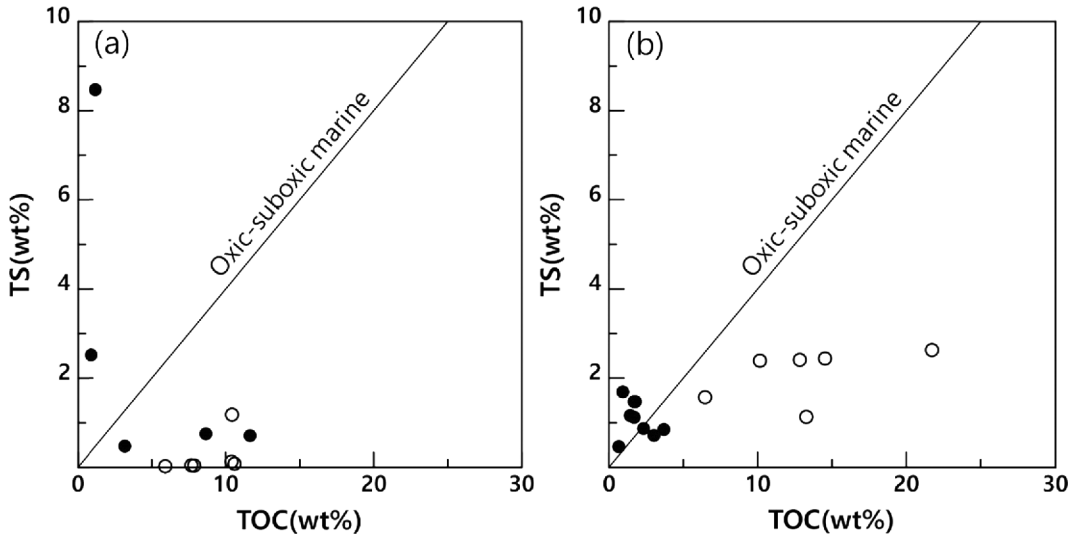

Fig. 10. TS (Total sulfur) versus TOC plots for the black and coaly slates from Boeun (a) and Geumsan (b) in the OMB.

addition, the enrichment of platinum group elements in the coaly slates was attributed to submarine hydrothermal activity (Shin and Kim, 2016). This raises the possibility that additional hydrothermal input of metals would have been accompanied as well.

As illustrated by U/Th ratios reflecting a hydrothermal effect for the coaly slates (Fig. 7), U can be concentrated in hydrothermal venting system (Bloch, 1980), because the anoxic condition established by a hydrothermal plume facilitates its accumulation in sediments as UO_2 via the reduction of U^{6+} to U^{4+}. It also has been revealed that exhalative particles in a hydrothermal plumes are important in the V scavenging from seawater (Trefry and Metz, 1989; Canet et al., 2004). Considering the highly enriched V concentration, up to 6,957 ppm, scavenging of V from seawater via hydrothermal exhalative oxide particles may represent an additional contribution to V enrichment in the coaly slates, adding to the distinctive enrichment of an anoxic sedimentation. Much higher Mo concentrations (avg. 170.2 ppm) with the occurrence of molybdenite crystals within the coaly slates (Jeong and Lee, 2001) than those in the black slates (avg. 5.5 ppm) of the OMB and in black shales elsewhere (i.e., 1.5 ppm according to Wedepohl, 1974) imply an additional source of Mo from hydrothermal venting. Unlike U, V, and Mo which are much more concentrated in the coaly slates, Cr, Co, and Ni are either less concentrated or depleted, which may be related to a relatively low concentration of reduced S species in the fluids (Leventhal, 1991). Nonetheless, a low concentration of base metals in the venting fluids cannot be ruled out.

It should be noted that different geochemical characteristics are noticed between the samples from two study areas in the OMB, such as stronger Eu anomaly for the coaly slates in Boeun (avg. 2.6) than Geumsan (avg. 1.6), higher P_2O_5 contents of the coaly slates in Geumsan (avg. 0.33 wt%) than Boeun (avg. 0.11 wt%), and larger difference of REE concentrations between the black slates and the coaly slates in Boeun (avg. 119 vs. 186 ppm) than Geumsan (avg. 175 vs. 191 ppm). These differences could reflect the local variances of redox conditions, source of metals, mineral occurrences, and relative contributions of metal enrichment process, etc. For example, the variance of P_2O_5 contents in the study area would have been controlled by the presence of apatite which commonly occurs as nodular form or in association with quartz, chlorite and uraninite in coaly slates (Jeong, 2006; Shin et al., 2016) (Fig. 3g). In addition to apatite, calcite which occurs as veinlet in both rock types (Figs. 3d and h) may have affected the variance of CaO contents in the study area as well. The relative abundances of monazite in both rock types (Shin et al., 2016) would also have contributed to different REE concentrations in two study areas.

TOC and S values for the samples from Geumsan tend to increase along the dysoxic to euxinic continuum, although the increase in TOC is much greater than that in S (Fig. 10b). The black slates are plotted in a comparatively narrow range around dysoxic facies, but the coaly slates are scattered toward euxinic facies. However, the samples from Boeun do not show systematic variations, but most of them are plotted close to the range of TOC threshold between anoxic (2.5 wt%) and euxinic (10 wt%) facies (Algeo and Maynard, 2004) (Fig. 10a). According to Arthur and Sageman (1994), however, despite the relatively high concentration of carbon, the low sulfur contents of the coaly slates indicate that the submarine depositional environment was likely to be dysoxic but not anoxic.

Anomalously enriched in S with low TOC is also noticeable in a sample of black slates from Boeun (Fig. 10a). Even though a

https://doi.org/10.1007/s12303-019-0018-7

loss of significant quantities of organic carbon by metamorphic effect could be suggested, considerably higher S contents compared to other samples would require other sources of the enrichments. Another possibility is an influx of H_2S produced by sulfate reduction from nearby black slates (Algeo and Maynard, 2004). However, such a local anomalous input for a sample seems to be unusual. The most likely explanation for the anomalous S enrichment is an excess of reactive iron in the system (Leventhal, 1993), which can be explained by hydrothermal input of reactive Fe (Pasava et al., 1996). Highest Fe content for the sample (7.52 wt% Fe_2O_3, PJ 22-1, Table 1) supports the interpretation. It seems like that the results of redox analysis by TOC-S relationships are somewhat different from those by trace elements-based facies assignment presented in Table 4. However, it has been asserted that redox analysis based on trace elements of strong euxinic affinity could yield more reliable results (Algeo and Maynard, 2004; Zhou and Jiang, 2009).

The black slate beds showing laterally extensive, thick, and high organic sediments in the OMB were interpreted to have originally formed in carbonaceous basins (Chough, 2013). And, the organic-rich metalliferous sediments were deposited in the basin under the influence of submarine hydrothermal activity related to rift setting (Cluzel et al., 1990; Kang et al., 2012). The occurrences of brecciated and flow textures, a sharp contact with the black slates, and nodular quartz veins accompanying intermittent massive sulfide aggregates in the coaly slates also support the idea that the metals were supplied directly from a hydrothermal vent, as they are similar to those developed in turbiditic sedimentation under submarine hydrothermal activities for black shales in South China (Steiner et al., 2001; Gu et al., 2012).

Thus it can be summarized that the metal enrichments in the coaly slates of the OMB seem to have been achieved in a similar way to those of the black shales in South China, as they are the results of combinations of direct hydrothermal input of metals into sediments under a reducing condition, probably proximal from the vent sites, hydrothermal scavenging of metals in the seawater, and the sorption of metals from seawater into organic-rich sediments as well (Fig. 11).

6. CONCLUSIONS

The redox-sensitive trace metal concentrations in the coaly slates in comparison with those in the black slates provide evidence of their depositional conditions in the OMB. Consistent higher V/(V + Ni), V/Cr, and U/Th ratios and depleted Mn contents in the coaly slates compared to those in the black slates indicate a strongly reducing environment for the formation of the metalliferous coaly slates, while the black slates may have been deposited under a suboxic-oxic condition. The REE patterns showing a positive Eu anomaly as well as a negative Ce anomaly are essentially inherited from submarine hydrothermal fluids under a reducing condition.

The concentrations of some redox-sensitive trace elements (V, Mo, U, and lower Cr) in the coaly slates are anomalously high compared to those in the black slates. The enrichment is inferred to have been controlled by direct hydrothermal input of metals into the rift basin from hydrothermal vents under a

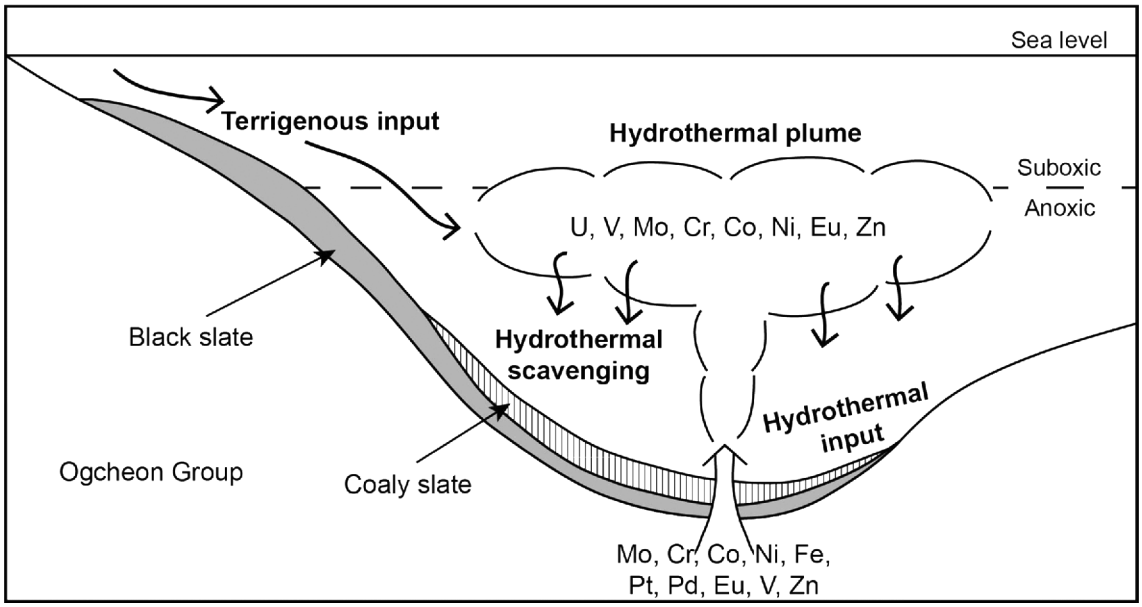

Fig. 11. Schematic illustration of depositional environment for metal enrichments in the OMB.

reducing condition, proximal from the vent sites, as supported by the textural evidences, and the metals could have been fixed from seawater by means of scavenging process via exhalative oxide particles in a hydrothermal plume. Additionally, it may have been influenced by the sorption of metals directly from seawater favored by anoxic conditions as evidenced by high TOC contents in the coaly slates. The metal enrichments in the metalliferous black slates of the OMB seem to have been achieved in a similar depositional environment to that of the black shales in South China.

ACKNOWLEDGMENTS

This work was supported by the research grant of the Kongju National University in 2017. We are grateful to the editor and anonymous reviewers for their valuable comments.

REFERENCES

Algeo, T.J. and Maynard, J.B., 2004, Trace-element behavior and redox facies in core shales of Upper Pennsylvanian Kansas-type cyclothems. Chemical Geology, 206, 289–318.

Anderson, R.F., Fleisher, M.Q., and Le Huray, A.P., 1989, Concentration, oxidation state and particulate flux of uranium in the Black Sea. Geochimica et Cosmochimica Acta, 53, 2215–2224.

Arthur, M.A. and Sageman, B.B., 1994, Marine black shales: depositional mechanisms and environments of ancient deposits. Annual Review of Earth and Planetary Sciences, 22, 499–551.

Baioumy, H. and Lehmann, B., 2017, Anomalous enrichment of redox-sensitive trace elements in the marine black shales from the Duwi Formation, Egypt: evidence for the Late Cretaceous Tethys anoxia. Journal of African Earth Sciences, 133, 7–14.

Bloch, S., 1980, Some factors controlling the concentration of uranium in the world ocean. Geochimica et Cosmochimica Acta, 44, 373–377.

Boström, K., 1983, Genesis of ferromanganese deposits-diagnostic criteria for recent and old deposits. In: Rona P.A., Boström K., Laubier L., and Smith K.L. (eds.), Hydrothermal Processes at Seafloor Spreading Centers. NATO Conference Series (IV Marine Sciences), Springer, Boston, 12, p. 473–489.

Canet, C., Alfonso, P., Melgarejo, J.C., and Belyatsky, B.V., 2004, Geochemical evidences of sedimentary-exhalative origin of the shale-hosted PGE-Ag-Au-Zn-Cu occurrences of the Prades mountains (Catalonia, Spain): trace-element abundances and Sm-Nd isotopes. Journal of Geochemical Exploration, 82, 17–33.

Carvalho, C., Anjos, R.M., Veiga, R., and Macario, K., 2011, Application of radiometric analysis in the study of provenance and transport processes of Brazilian coastal sediments. Journal of Environmental Radioactivity, 102, 185–192.

Chang, E.Z., 1996, Collisional orogene between North and South China and its eastern extension in the Korean peninsula. Journal of Southeastern Asian Earth Sciences, 13, 267–277.

Cheong, C.S., Jeong, G.Y., Kim, H., Choi, M.S., Lee, S.H., and Cho, M., 2003, Early Permian peak metamorphism recorded in U-Pb system of black slates from the Ogcheon metamorphic belt, South Korea, and its tectonic implication. Chemical Geology, 193, 81–92.

Choi, D.K., Woo, J., and Park, T.Y., 2012, The Okcheon Supergroup in Lake Chungju area, Korea: Neoproterozoic volcanic and glaciogenic sedimentary succession in a rift basin. Geosciences Journal, 12, 207–227.

Chough, S.K., 2013, Geology and sedimentology of the Korean Peninsula. Elsevier, Amsterdam, 363 p.

Cluzel, D., Cadet, J.P., and Lapierre, H., 1990, Geodynamics of the Ogcheon belt (South Korea). Tectonophysics, 183, 41–56.

Coveney, R.M. Jr., 2003, Re-Os dating of polymetallic Ni-Mo-PGE-Au mineralization in Lower Cambrian black shales of South China and its geological significance – a discussion. Economic Geology, 98, 661–662.

Craddock, P.R., Bach, W., Seewald, J.S., Rouxel, O.J., Reeves, E., and Tivey, M.K., 2010, Rare earth element abundances in hydrothermal fluids from the Manus basin, Papua New Guinea: indicators of sub-seafloor hydrothermal processes in back-arc basins. Geochimica et Cosmochimica Acta, 74, 5494–5513.

Degens, E.T., Williams, E.G., and Keith, E.G., 1958, Application of geochemical criteria [Pennsylvania], Part 2 of environmental studies of Carboniferous sediments. American Association of Petroleum Geologists Bulletin, 42, 981–997.

Elderfield, H. and Greaves, M.J., 1982, The rare earth elements in seawater. Nature, 296, 214–219.

Fleurance, S., Cuney, M., Malartre, F., and Reyx, J., 2013, Origin of the extreme polymetallic enrichment (Cd, Cr, Mo, Ni, U, V, Zn) of the Late Cretaceous–Early Tertiary Belqa Group, central Jordan. Palaeogeography, Palaeoclimatology, Palaeoecology, 369, 201–219.

Francois, R., 1988, A study on the regulation of the concentrations of some trace metals (Rb, Sr, Zn, Pb, Cu, V, Cr, Ni, Mn and Mo) in Saanich inlet sediments, British Columbia, Canada. Marine Geology, 83, 285–308.

German, C.R. and Elderfield, H., 1990, Application of the Ce anomaly as paleoredox indicator: the ground rules. Paleooceanography, 5, 823–833.

Gromet, L.P., Dymek, R.F., Haskin, L.A., and Korotev, R.L., 1984, The "North American Shale Composite": its compilation, major and trace element characteristics. Geochimica et Cosmochimica Acta, 48, 2469–2482.

Gu, X.X., Zhang, Y.M., Schulz, O., Vavtar, F., Liu, J.M., Zheng, M.H., and Zheng, L., 2012, The Woxi W-Sb-Au deposit in Hunan, South China: an example of Late Proterozoic sedimentary exhalative (SEDEX) mineralization. Journal of Asian Earth Sciences, 57, 54–75.

Hatch, J.R. and Leventhal, J.S., 1992, Relationship between inferred redox potential of the depositional environment and geochemistry of the Upper Pennsylvanian (Missourian) Stark Shale Member of the Dennis Limestone, Wabaunsee County, Kansas, U.S.A. Chemical Geology, 117, 287–302.

Hild, E. and Brumsack, H.-J., 1998, Major and minor element geochemistry of Lower Aptian sediments from the NW German basin (Core Hoheneggelsen KB 40). Cretaceous Research, 19, 615–633.

Hiroi, Y., 1983, Progressive metamorphism of the Unazaki pelitic schists in the Hida Terrane, Central Japan. Contributions to Mineralogy

 https://doi.org/10.1007/s12303-019-0018-7

and Petrology, 82, 334–350.
Jeong, G.Y., 2006, Mineralogy and geochemistry of metalliferous black slates in the Okcheon metamorphic belt, Korea: a metamorphic analogue of black shales in the South China block. Mineralium Deposita, 41, 469–481.
Jeong, G.Y. and Lee, S.H., 2001, Form of molybdenum in the carbonaceous black slates of the Ogcheon belt. Journal of the Mineralogical Society of Korea, 14, 52–57. (in Korean with English abstract)
Jiang, S.Y., Chen, Y.Q., Ling, H.F., Yang, J.H., Feng, H.Z., and Ni, P., 2006, Trace- and rare-earth element geochemistry and Pb-Pb dating of black shales and intercalated Ni-Mo-PGE-Au sulfide ores in Lower Cambrian strata, Yangtze Platform, South China. Mineralium Deposita, 41, 453–467.
Jiang, S.Y., Pi, D.H., Heubeck, C., Frimmel, H., Liu, Y.P., Deng, H.L., Ling, H.F., and Yang, J.H., 2009, Early Cambrian ocean anoxia in South China. Nature, 459, E5–E6.
Jo, N.H., Shin, D.B., Kim, C.R., and Yi, M.J., 2013, Geology and geochemical characteristics of uranium mineralized zone in Suyoung area, Geumsan. Journal of the Geological Society of Korea, 49, 231–244. (in Korean with English abstract)
Jones, B. and Manning, D.A.C., 1994, Comparison of geochemical indices used for the interpretation of depositional environments in ancient mudstones. Chemical Geology, 111, 112–129.
Kang, J.H., Hayasaka, Y., and Ryoo, C.R., 2012, Tectonic evolution of the central Ogcheon belt, Korea. Journal of the Petrological Society of Korea, 21, 129–150. (in Korean with English abstract)
Kim, J.H., 1989, Geochemistry and genesis of Guryongsan (Ogcheon) uraniferous black slate. Journal of the Korean Institute of Mining Geology, 22, 35–63. (in Korean with English abstract)
Kim, Y.J., Seo, J., Kang, S.A., Choi, S.G., and Lee, Y.J., 2015, Geochemistry and uranium mineralogy of the black slate in the Okcheon metamorphic belt, South Korea. Geochemical Journal, 49, 443–452.
Klinkhammer, G., Elderfield, H., and Hudson, A., 1983, Rare earth elements in seawater near hydrothermal vents. Nature, 305, 185–188.
Kunzmann, M., Halverson, G.P., Scott, C., Minarik, W.G., and Wing, B.A., 2015, Geochemistry of Neoproterozoic black shales from Svalbard: implications for oceanic redox conditions spanning Cryogenian glaciations. Chemical Geology, 417, 383–393.
Kwon, S.T. and Lan, C.Y., 1991, Sm-Nd isotopic study of the Ogcheon amphibolite, Korea: preliminary report. Journal of the Korean Institute of Mining Geology, 24, 277–285. (in Korean with English abstract)
Lee, C.H. and Lee, H.K., 1997, Geochemistry and mineralogy of metapelite and barium-vanadium muscovite from the Ogcheon Supergroup of the Deokpyeong area, Korea. Economic and Environmental Geology, 30, 35–49.
Lee, D.S., Yun, S.K., Lee, J.H., and Kim, J.T., 1986, Lithologic and structural controls and geochemistry of uranium deposition in the Ogcheon black-slate formation. Journal of the Korean Institute of Mining Geology, 19, 19–41. (in Korean with English abstract)
Lee, K.S., Chang, H.W., and Park, K.H., 1998, Neoproterozoic bimodal volcanism in the central Ogcheon belt, Korea: age and tectonic implication. Precambrian Research, 89, 47–57.
Lehmann, B., Frei, R., Xu, L., and Mao, J., 2016, Early Cambrian black shale-hosted Mo-Ni and V mineralization on the rifted margin of the Yangtze Platform, China: reconnaissance chromium isotope data and a refined metallogenic model. Economic Geology, 111, 89–103.
Lehmann, B., Nägler, T.F., Holland, H.D., Wille, M., Mao, J.W., Pan, J.Y., Ma, D.S., and Dulski, P., 2007, Highly metalliferous carbonaceous shale and Early Cambrian seawater. Geology, 35, 403–406.
Leventhal, J.S., 1991, Comparison of organic geochemistry and metal enrichment in two black shales: Cambrian Alum shale and Devonian Chattanooga shale of United States. Mineralium Deposita, 26, 104–112.
Leventhal, J.S., 1993, Metals in black shales. In: Engel, M.H. and Macko, S.A. (eds.), Organic Geochemistry: Principles and Applications. Plenum Press, New York, p. 581–592.
Lott, D.A., Coveney, R.M., Murowchick, J.B., and Grauch, R.I., 1999, Sedimentary exhalative nickel-molybdenum ores in South China. Economic Geology, 94, 1051–1066.
Mao, J., Lehmann, B., Du, A., Zhang, G., Ma, D., Wang, Y., Zeng, M., and Kerrich, R., 2002, Re-Os dating of polymetallic Ni-Mo-PGE-Au mineralization in Lower Cambrian black shales of South China and its geologic significance. Economic Geology, 97, 1051–1061.
Michard, A. and Albarede, F., 1986, The REE content of some hydrothermal fluids. Chemical Geology, 55, 51–60.
Michard G., Albarède F., Michard A., Minster J.F., and Charlou J.L., 1983, Rare-earth elements and uranium in high-temperature solutions from East Pacific Rise hydrothermal vent field (13°N). Nature, 303, 795–797.
Min, K. and Cho, M., 1998, Metamorphic evolution of the northwestern Ogcheon metamorphic belt, South Korea. Lithos, 43, 31–51.
Morford, J.L. and Emerson, S., 1999, The geochemistry of redox sensitive trace metals in sediments. Geochimica et Cosmochimica Acta, 63, 1735–1750.
Parr, J.M., 1992, Rare-earth element distribution in the exhalites associated with Broken Hill-type mineralization at the Pinacles deposit, New South Wales, Australia. Chemical Geology, 100, 73–91.
Pasava, J., Hladikova, J., and Dobes, P., 1996, Origin of Proterozoic metal-rich black shales from the Bohemian Massif, Czech Republic. Economic Geology, 91, 63–79.
Pasava, J., Kribek, B., Vymazalova, A., Sykorova, I., Zak, K., and Orberger, B., 2008, Multiple sources of metals of mineralization in Lower Cambrian black shales of South China: evidence from geochemical and petrographic study. Resource Geology, 58, 25–42.
Pattan, J.N., Pearce, N.J.G., and Mislankar, P.G., 2005, Constraints in using cerium-anomaly of bulk sediments as an indicator of paleo bottom water redox environment: a case study from the Central Indian ocean basin. Chemical Geology, 221, 260–278.
Pi, D.H., Liu, C.Q., Shields-Zhou, G.A., and Jiang, S.Y., 2013, Trace and rare earth element geochemistry of black shale and kerogen in the Early Cambrian Niutitang formation in Guizhou province, South China: constraints for redox environments and origin of metal enrichments. Precambrian Research, 225, 218–229.
Pi, D.H., Jiang, S.H., Luo, L., Yang, J.H., and Ling, H.F., 2014, Depositional environments for stratiform witherite deposits in the Lower Cambrian black shale sequence of the Yangtze platform, southern Qinling region, SW China: evidence from redox-sensitive trace element geochemistry. Palaeogeography, Palaeoclimatology, Palaeoecology, 398, 125–131.
Quinby-Hunt, M.S. and Wilde, P., 1994, Thermodynamic zonation in

the black shale facies based on iron-manganese-vanadium content. Chemical Geology, 113, 297–317.

Ree, J.H., Kwon, S.H., Park, Y.D., Kwon, S.T., and Park, S.H., 2001, Pretectonic and post-tectonic emplacements of the granitoids in the south central Okcheon belt, South Korea: implications for the timing of strike-slip shearing and thrusting. Tectonics, 20, 850–867.

Shields, G. and Stille, P., 2001, Diagenetic constrains on the use of cerium anomalies as palaeoseawater proxies: an isotopic and REE study of Cambrian phosphorites. Chemical Geology, 175, 29–48.

Shin, D.B. and Kim, S.J., 2011, Geochemical characteristics of black slate and coaly slate from the uranium deposit in Deokpyeong Area. Economic and Environmental Geology, 44, 373–386. (in Korean with English abstract)

Shin, D.B. and Kim, S.J., 2016, PGE distribution in the metalliferous black slates of the Okcheon metamorphic belt, South Korea. Geosciences Journal, 20, 827–835.

Shin, I.K., Kim, S.H., and Shin, D.B., 2016, Mineralogy and sulfur isotope compositions of the uraniferous black slates in the Ogcheon metamorphic belt, South Korea. Journal of Geochemical Exploration, 169, 1–12.

Slack, J.F., Dumoulin, J.A., Schmidt, J.M., Young, L.E., and Rombach, C.S., 2004, Paleozoic sedimentary rocks in the Red Dog Zn-Pb-Ag district and vicinity, western Brooks Range, Alaska: provenance, deposition, and metallogenic significance. Economic Geology, 99, 1385–1414.

Sotto, D. and Yoshiyuki, N., 1999, Rare earth elements in seawater: particle association, shale normalization, and Ce oxidation. Geochimica et Cosmochimica Acta, 63, 363–372.

Steiner, M., Wallis, E., Erdtmann, B.D., Zhao, Y.L., and Yang, R.D., 2001, Submarine-hydrothermal exhalative ore layers in black shales from South China and associated fossils: insights into a Lower Cambrian facies and bio-evolution. Palaeogeography, Palaeoclimatology, Palaeoecology, 169, 165–191.

Suzuki, K. and Adachi, M., 1994, Middle Precambrian detrital monazite and zircon from the Hida belt gneiss on Oki-Dogo island, Japan: their origin and implications for the correlation of basement gneiss of southwest Japan and Korea. Tectonophysics, 235, 277–292.

Trefry, J.H. and Metz, S., 1989, Role of hydrothermal precipitates in the geochemical cycling of vanadium. Nature, 342, 531–533.

Tribovillard, N., Algeo, T.J., Lyons, T., and Riboulleau, A., 2006, Trace metals as paleoredox and paleoproductivity proxies: an update. Chemical Geology, 232, 12–32.

Wedepohl, K.H., 1974, Handbook of Geochemistry. Springer, Berlin, 442 p.

Wignall, P.B., 1994, Black Shales. Clarendon Press, Oxford, 127 p.

Xu, L.G., Lehmann, B., and Mao, J.W., 2013, Seawater contribution to polymetallic Ni-Mo-PGE-Au mineralization in Early Cambrian black shales of South China: evidence from Mo isotope, PGE, trace element, and REE geochemistry. Ore Geology Reviews, 52, 66–84.

Young, S.A., Loukola-Ruskeeniemi, K., and Pratt, L.M., 2013, Reactions of hydrothermal solutions with organic matter in Paleoproterozoic black shales at Talvivaara, Finland: evidence from multiple sulfur isotopes. Earth and Planetary Science Letters, 367, 1–14.

Zhao, J., Jin, Z., Jin, Z., Geng, Y., Wen, X., and Yan, C., 2016, Applying sedimentary geochemical proxies for paleoenvironment interpretation of organic-rich shale deposition in the Sichuan basin, China. Internation Journal of Coal Geology, 163, 52–71.

Zhou, C.M. and Jiang, S.Y., 2009, Palaeoceanographic redox environments for the Lower Cambrian Hetang formation in South China: evidence from pyrite framboids, redox-sensitive trace elements, and sponge biota occurrence. Palaeogeography, Palaeoclimatology, Palaeoecology, 271, 279–286.

https://doi.org/10.1007/s12303-019-0018-7